

Representations of the Renormalization Group as Matrix Lie Algebra

M. Berg^{1 2}

*Center for Relativity
University of Texas at Austin, USA*

P. Cartier

*Département de Mathématiques et Applications
Ecole Normale Supérieure, Paris, France*

Abstract

Renormalization is cast in the form of a Lie algebra of matrices. By exponentiation, these matrices generate counterterms for Feynman diagrams with subdivergences. The matrices are triangular, and in general infinite. As representations of an insertion operator, the matrices provide explicit representations of the Connes-Kreimer Lie algebra. In fact, the right-symmetric nonassociative algebra of the Connes-Kreimer insertion product is equivalent to an “Ihara bracket” in the matrix Lie algebra. We check our results in a few three-loop examples in scalar field theory. Apart from the obvious application to high-precision phenomenology, some ideas about possible applications in noncommutative geometry and functional integration are given.

¹This work was partially performed while visiting DMA, Ecole Normale Supérieure.

²Email contact: mberg@physics.utexas.edu

1 Introduction

It has been known for several years now that renormalization is governed by certain algebras known as Hopf algebras (for a review, see Kreimer [30]). Unfortunately, since Hopf algebra is largely unfamiliar to physicists³, this intriguing fact has not been widely appreciated. Here, we make an attempt to help remedy this situation, by focusing instead on an equivalent Lie algebra. The existence of such a Lie algebra is guaranteed by the famous Milnor-Moore theorem [10, 20], a fact that was exploited by Connes and Kreimer already in [19]. This theorem says, loosely speaking, that any graded Hopf algebra can be written in terms of a Lie algebra. The mere fact that Lie algebra is much more familiar to physicists than Hopf algebra makes this direction useful to explore. In addition, there are certain computational advantages that may prove important; the Lie algebra can be expressed in terms of (in general infinite) matrices, so renormalization becomes a matter of matrix algebra. The matrix Lie algebra is the subject of this work. We explore the application to renormalization and give a number of examples.

Via the homomorphism between the Hopf algebra of renormalization and the Hopf algebra of coordinates on the group of formal diffeomorphisms in noncommutative geometry [20, 22], we also expect to be able to apply the matrix framework in noncommutative geometry terms, but this direction is postponed to future work. (Reasons why noncommutative geometry could be relevant to physics abound [9, 18, 33, 37].) There is also another, more speculative way in which this matrix Lie algebra may be applied, explained in the conclusion, section 10. First, let us step back and review some existing directions in the literature. Partly through indications of recommended references, we will attempt to maintain some accessibility for mathematicians who are not completely familiar with physics jargon.

2 Background

Perturbative renormalization was regarded by most physicists as finished with a theorem by Bogoliubov, Parasiuk, Hepp, and Zimmermann (the BPHZ theorem), refined by Zimmermann in 1970. Original references for this theorem are [2], and a clear textbook version is given in [16]. Already hidden within the BPHZ theorem, however, was algebraic structure belonging to branches of mathematics that were probably largely unknown to physicists in

³except in completely different contexts, as symmetries of some nonlinear sigma models in low-dimensional supergravity. A basic Hopf algebra reference is [26].

the 1970s. The Hopf algebra of renormalization was first displayed by Kreimer in 1997, partially as a result of his excursions into knot theory [28]. In 1999, Broadhurst and Kreimer performed a Hopf-algebraic show of strength by computing contributions to anomalous dimensions in Yukawa theory to 30 loops [4]⁴.

On a practical level, phenomenologists have been opening their eyes to Hopf algebra as a potential time-saver and organizing principle in massive computations, such as the 5-loop computation of the beta function in quantum chromodynamics (QCD). Such high-precision analytical calculations are needed for comparisons to numerical calculations in lattice QCD, since the energy scales accessible in these lattice computations (and in many experiments) are often so low that perturbative QCD is only starting to become a valid approximation (see e.g. [1, 12]). Even when one is not seeking to push calculations to such heights of precision, savings in computer time through better algorithms could be welcome for routine calculations as well.

On the more mathematical side, a series of articles by Connes and Kreimer [19, 20] took the Hopf algebra of renormalization through some formal developments, amongst other the identification of the Lie algebra of the dual of the aforementioned Hopf algebra, through the Milnor-Moore theorem (see also [10] for more recent mathematical developments). This has later been phrased as a study of *operads*⁵ [32], which we will not go into here, but which can be seen as complementary to our discussion. Very recently, some geometric aspects were explored in [14].

We believe that representations of the dual Lie algebra can be useful in their own right, so this work is about one such representation. The Lie bracket is simply given by inserting one graph into another, and subtracting the opposite insertion. The process of insertion may be represented by the multiplication of (in general infinite) matrices, hence matrix Lie algebra.

Although we give examples in scalar field theory, the algebra representation on graphs is independent of the specific nature of the action, except that we assume the interactions are quartic. We could equally well consider fermions, vector fields, or higher-spin fields with quartic interactions. But surely Ward identities, ghosts and so on make gauge theory computations very different from those of scalar field theory? This question can be answered on two levels. First, the distinction between Feynman graphs and their values. In performing

⁴This was later improved further [5].

⁵For instance, a simple example of an operad is a collection of maps from all tensor products of an algebra \mathcal{A} into \mathcal{A} itself, such as $\mathcal{A} \otimes \mathcal{A} \otimes \mathcal{A} \rightarrow \mathcal{A}$, with some compatibility requirements. See e.g. [27] for a precise definition.

field theory computations, one routinely identifies graphs and their values. In the Connes-Kreimer approach one explicitly separates symmetries of the algebra of Feynman graphs from symmetries of Feynman integrals; the integrals are thought of as elements of the dual of the space of graphs. The dual has symmetries of its own, “quasi-shuffles” [29], obviously related but not identical to symmetries on graphs. The algebraic approach can help with computing Feynman integrals, but its greatest strengths so far has been in the organization of counterterms, providing algebraic relations between seemingly unrelated quantities. The organization of counterterms is an essentially graph-theoretic problem, since the hierarchy of subdivergences can be read off from the topology of a graph without knowing precisely what fields are involved. In the extreme case of “rainbow” or “ladder” diagrams only, the Feynman integrals themselves are easily iterated to any loop order (as in [4]), but the BPHZ subtractions quickly become a combinatorial mess if the algebraic structure is ignored.

The attitude of separating the combinatorial and analytical problems (space of graphs and its dual) is also useful for computer implementation. Let us take one example: the Mathematica package *FeynArts* [24], which can automatically compute amplitudes up to one loop in any renormalizable theory, and using additional software, up to two loops [25]. This particular software package calculates amplitudes by first writing down scalar graphs with appropriate vertices, then generates counterterm graphs, then at a later stage lets the user specify what fields are involved, either gauge fields, spinors or scalars. Since the number of graphs grows very quickly with loop order, it will become important to take advantage of algebraic structure if calculations at very high precision are to be feasible in a reasonable amount of computer time.

Apart from the direct application of the matrix Lie algebra to precision computations, there are other possible indirect applications. Such applications may be found in noncommutative geometry through the result of [20]. A currently more speculative application is to functional integration. These directions are not explored in detail in this work, but see section 10.

3 Graph Summary

We consider ϕ^4 theory in four spacetime dimensions for ease of exposition (see the previous section for comments on adaption to other theories). In ϕ^4 theory in four dimensions, we consider graphs with a quartic interaction vertex⁶ and two and four external legs (see section

⁶i.e. the interaction vertex is four-valent.

L	E	Graphs									
0	2	—									
0	4										
1	2										
1	4		(
2	2										
2	4					+ crossing					
3	2										
3	4										
								+ crossing			

Table 1: Graphs with L loops and E external legs.

9 for a reminder of why we do not need e.g. six external legs in this theory in four dimensions). All such graphs with up to three loops are summarized in table 1⁷. In this table, “crossing” refers to graphs related to previously given graphs by crossing symmetry, such as the two graphs in parenthesis for $L = 1$, $E = 4$; they are simply found by turning the first graph on its side (second graph), and then crossing the two lower external legs (third graph).⁸ On a computer, graphs can be stored as lists. One example of such lists, adapted to the context of Feynman graphs, is given at the end of section 4.

4 The Grafting Operator

The Lie algebra of graphs comes from inserting (grafting) one Feynman graph into another. First a remark about terminology. In standard Feynman graphs, each internal line represents a propagator. We will only work with amputated graphs, where the external legs do not represent propagators. Now, in a theory with quartic interactions, one can consider inserting graphs with either two external legs (into an internal line) or four external legs (into an interaction vertex). Thus, the middle of an internal line and the interaction vertex itself are eligible as *insertion points*. If desired, we could represent each insertion point by a dot, as

⁷These graphs were drawn using FeynMF [35].

⁸The reader unfamiliar with Feynman diagrams may want to note that the third graph in $L = 1$, $E = 4$ still has only two vertices: the two lines crossing below the loop are going one above the other.

in the graph on the left in fig. 1. As in standard usage—the graph on the right in fig. 1—we leave those dots implicit. We alert the reader that the authors of [19] call the dots on lines

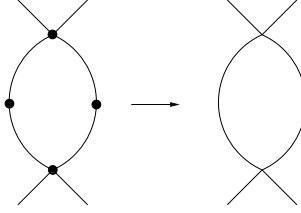


Figure 1: Insertion points are implicit.

“two-point vertices”. To avoid confusion with standard physics terminology, we prefer to talk about insertion points, and we will not talk about two-point vertices.

Here is a precise definition of the insertion, or grafting, operator. The practically-minded reader can refer to the insertion tables in appendix A to get a quick idea of the action of this operator. Enumerate the insertion points of a graph t by $p_i(t)$, the total number of insertion points of t by $N(t)$ and their valences (number of “prongs”, i.e. lines sticking out from the vertex) by $v(p_i(t))$. Here, the valence is always either 2 or 4. If t_1 and t_2 are graphs, and the number $v(t_2)$ of external legs of t_2 is equal to the valence $v(p_i(t_1))$ of the insertion point $p_i(t_1)$ of t_1 , then we define $s_{t_2}^{p_i(t_1)}$ to be insertion of the graph t_2 at $p_i(t_1)$ by summing over all permutations of the $v(p_i(t_1))$ propagators to be joined. Then the grafting operator s_{t_2} is

$$s_{t_2} t_1 = \frac{1}{v(t_2)!} \sum_{i=1}^{N(t_1)} s_{t_2}^{p_i(t_1)} t_1 . \quad (1)$$

The total number of graphs \mathcal{N} (including multiplicities of the same graph) created by insertion of t_2 into t_1 is

$$\mathcal{N} = \sum_{i=1}^{N(t_1)} \delta_{v(p_i(t_1)), v(p_i(t_2))} v(p_i(t_1))!$$

We call t_1 the “object graph” and t_2 the “insertion graph”. Often, we will use parenthesis to delineate the insertion graph: $s(t_2)t_1$. Finally, we define $s(t)$ to be linear:

$$s(at_1 + bt_2) = as(t_1) + bs(t_2) \quad a, b \in \mathbb{C} .$$

A remark about normalization: the normalization in (1) is a mean over insertions. It gives $s_t 1 = t$, where 1 represents tree-level graphs, with either 2 or 4 external legs. (When one

needs to make a distinction, one can use 1_2 and 1_4 .) On the other hand, we have $s_1 t \neq t$, in fact

$$s_1 t = N(t) t = (3L(t) \pm 1) t \quad (t \neq 1)$$

where $L(t)$ is the number of loops of t and the upper (lower) sign refers to graphs with 4 (2) external legs, respectively.

We can assign a grading (degree) to the algebra by loop number L , since then obviously

$$\deg s_{t_2} t_1 = \deg t_2 + \deg t_1 ,$$

so within the set of graphs with a fixed number of external legs, s_1 acts as our grading operator. Being the only s_t which is diagonal, we will exclude s_1 from the algebra, but it can be adjoined whenever needed as in [20].

4.1 Overlapping divergences

It is of particular interest to know when a graph has overlapping divergences, i.e. when two loops share the same propagator. For any graph, two lines are said to be indistinguishable if they are connected to the same vertex, and distinguishable if they are not. Whenever we insert a (loop) graph with four external legs at a certain vertex and two distinguishable external prongs of the insertion graph are connected to indistinguishable legs of another vertex, we create overlapping divergences. Of course, any overlapping divergences already present in the insertion graph are preserved.

Here is an example. Consider the insertion in fig. 2. It is an insertion of \mathfrak{X} into the upper vertex of that same graph. With the above use of language, 5 and 6 are equivalent, and so are 9 and 10, but not e.g. 5 and 7. When we join 3-5, 4-6, 7-9, 8-10, we create \mathfrak{Y} . But when we join 3-5, 4-8, 7-9, 6-10, we create \mathfrak{Z} , which has overlapping divergences.

As a side remark, figure 2 also lets us recall how \mathfrak{X} is easily represented in a format amenable to computer processing. The bottom vertex can be stored as [9, 10, 11, 12], and the propagator going between 5 and 7 carrying loop momentum p can be stored as [5, 7, p]. This way, the list of vertices contains three sublists, and the list of propagators contains four sublists, which together completely specify the graph. This is also how graphs are stored in *FeynArts* [24]. Of course, there are many other equivalent representations, for instance using the relation between rooted trees and parenthesized words [3].

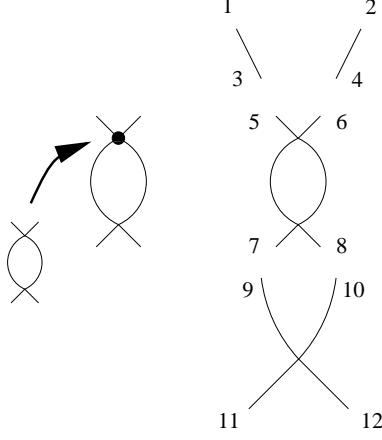


Figure 2: The creation of overlapping divergences

5 Lie Algebra

We want to show that the grafting operators s_t form a Lie algebra \mathcal{L} . To this end, we first show a certain operator identity. Indeed for graphs t_1, t_2 , define

$$[t_1, t_2] = s(t_1)t_2 - s(t_2)t_1 \quad (2)$$

then we shall show that the commutator of the operators $s(t_1), s(t_2)$ is equal to $s([t_1, t_2])$:

$$[s(t_1), s(t_2)] = s([t_1, t_2]) , \quad (3)$$

as an operator identity acting on graphs. This identity is analogous to the Ihara bracket of the Magnus group, familiar from number theory (see e.g. [36]).

Here is a sketch of the proof of (3). Consider two insertions into a graph t_3 , $s_{t_1}^{p_i(t_3)}$ and $s_{t_2}^{p_j(t_3)}$, before summing over insertion points $p_i(t_3)$ and $p_j(t_3)$. Let us separate insertions into “mutually local” (if $p_i(t_3) = p_j(t_3)$) and “mutually nonlocal” (otherwise). This is illustrated in figure 3. The “mutually nonlocal” insertions clearly commute, since they modify different points, so these contributions to s_{t_1} and s_{t_2} cancel in the bracket. We are left with the “local” insertions, i.e.

$$s_{t_1}t_2 - s_{t_2}t_1 =: [t_1, t_2]$$

This concludes the outline of the proof. Using the correspondence in section 5.1, a detailed proof will appear in [6].

We remark that the identity trivially holds acting on 1:

$$[s(t_1), s(t_2)]1 = s(t_1)s(t_2)1 - s(t_2)s(t_1)1 = s(t_1)t_2 - s(t_2)t_1 = [t_1, t_2] .$$

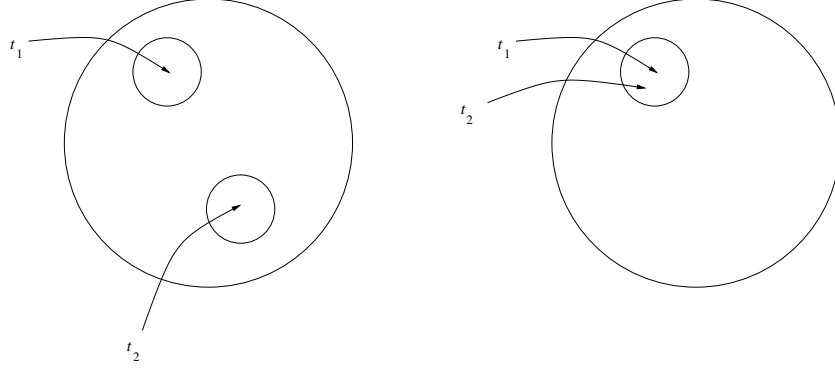


Figure 3: Difference between mutually nonlocal (a) and mutually local insertions (b).

It is easy to check that the bracket $[t_1, t_2] = s(t_1)t_2 - s(t_2)t_1$ satisfies the Jacobi identity. By writing down three copies of the Ihara bracket identity (3) and adding them we find by linearity

$$s([t_1, t_2])t_3 + s(t_3)[t_2, t_1] + \text{cyclic} = 0$$

or

$$[t_1, [t_2, t_3]] + \text{cyclic} = 0 .$$

The Lie algebra is graded by loop order: $\mathcal{L} = \mathcal{L}^{(1)} \oplus \mathcal{L}^{(2)} \oplus \mathcal{L}^{(3)} \oplus \dots$ and

$$[\mathcal{L}^{(m)}, \mathcal{L}^{(n)}] \subset \mathcal{L}^{(m+n)} .$$

Let us see what the Lie bracket looks like explicitly in our field theory with four-vertices. To make the notation more economic, we suppress any graph which is related by crossing symmetry to one that is already included. That is, since $\text{\text{X}}$, $\text{\text{X}}$ and $\text{\text{X}}$ (see table 1) all represent the same function of the different Mandelstam variables⁹ s , t , and u , we will only display $\text{\text{X}}$ out of those three diagrams. We can always use a symmetric renormalization point, i.e. we can define the theory at some mass scale M , meaning $s = t = u = -M^2$ at this scale, in which case counterterms are the same for all three diagrams mentioned previously.

At the one-loop level, we have the following diagrams: --- , $\text{\text{X}}$, $\text{\text{X}}$ and $\text{\text{X}}$. Consulting the insertion tables in the appendix, or equivalently the matrix representation which we introduce below, we find the commutators of tree-level diagrams with one-loop diagrams:

$$[\mathcal{L}^{(0)}, \mathcal{L}^{(1)}] \subset \mathcal{L}^{(1)} :$$

⁹Here $s = (p_1 + p_2)^2$, $t = (p'_1 - p_1)^2$ and $u = (p'_2 - p_1)^2$, where p_1, p_2 are incoming momenta, and p'_1, p'_2 are outgoing momenta.

$$\begin{aligned}
[-, \underline{\mathcal{O}}] &= s(-)\underline{\mathcal{O}} - s(\underline{\mathcal{O}})- \\
&= 2\underline{\mathcal{O}} - \underline{\mathcal{O}} \\
&= \underline{\mathcal{O}} \\
[\times, \mathfrak{X}] &= s(\times)\mathfrak{X} - s(\mathfrak{X})\times \\
&= 2\mathfrak{X} - \mathfrak{X} \\
&= \mathfrak{X}.
\end{aligned}$$

The only nonvanishing commutator of two one-loop graphs is

$$\begin{aligned}
[\mathcal{L}^{(1)}, \mathcal{L}^{(1)}] &\subset \mathcal{L}^{(2)} : \\
[\mathfrak{X}, \underline{\mathcal{O}}] &= s(\mathfrak{X})\underline{\mathcal{O}} - s(\underline{\mathcal{O}})\mathfrak{X} \\
&= \frac{1}{3}\underline{\mathfrak{X}} + \frac{2}{3}\Theta - 2\mathfrak{X} \xrightarrow{I} \mathcal{O}(\hbar). \tag{4}
\end{aligned}$$

where by \xrightarrow{I} we mean evaluation of the graphs. Here we have restored \hbar to connect with the semiclassical approximation; an L -loop graph is of order \hbar^{L-1} . At this point we note that the combinatorial factors $1/3$, $2/3$ and so on are *not* the usual symmetry factors of graphs, i.e. the multiplicity of operator contractions generating the same graph.

Including two-loop graphs in the algebra, the following graphs come into play: \mathfrak{X} , \mathfrak{X} , \mathfrak{X} and \mathfrak{X} . We can now consider a commutator of a one-loop and a two-loop graph, which creates a sequence of three-loop graphs:

$$\begin{aligned}
[\mathcal{L}^{(1)}, \mathcal{L}^{(2)}] &\subset \mathcal{L}^{(3)} : \\
[\mathfrak{X}, \mathfrak{X}] &= s(\mathfrak{X})\mathfrak{X} - s(\mathfrak{X})\mathfrak{X} \\
&= \frac{2}{3}\mathfrak{X} + \frac{2}{3}\mathfrak{X} + \frac{2}{3}\mathfrak{X} \\
&\quad - \frac{2}{3}\mathfrak{X} - \mathfrak{X} - \frac{2}{3}\mathfrak{X} - \frac{2}{3}\mathfrak{X} \\
&\xrightarrow{I} \mathcal{O}(\hbar^2),
\end{aligned}$$

which may be approximated by zero if we only keep graphs up to order \hbar . Thus, to this order, all the “new” graphs with two loops are central elements of the algebra.

In general, if we consider L loops (order \hbar^{L-1}), the commutator at order \hbar^L is negligible, so only commutators of graphs of loop orders L_1, L_2 where $L_1 + L_2 \leq L$ are nonvanishing. The effect of going from L to $L + 1$ is then to add central graphs as new generators, which appear in lower-order commutators with one extra factor of \hbar . In other words, the new graphs *deform* the L -loop algebra by \hbar .

Now that we have displayed a few commutators, here are two examples of how the Ihara bracket identity works. Let us first consider a one-loop/one-loop commutator, acting on the bare propagator.

$$\begin{aligned}
s([\varnothing, \ominus]) - &= s(s(\varnothing)\ominus) - s(s(\ominus)\varnothing) - \\
&= s\left(\frac{1}{3}\varnothing + \frac{2}{3}\ominus\right) - \\
&= \frac{1}{3}s(\varnothing) - + \frac{2}{3}s(\ominus) - \\
&= \frac{1}{3}\varnothing + \frac{2}{3}\ominus
\end{aligned}$$

whereas



$$\begin{aligned}
[s(\varnothing), s(\ominus)] - &= s(\varnothing)s(\ominus) - s(\ominus)s(\varnothing) - \\
&= s(\varnothing)\ominus \\
&= \frac{1}{3}\varnothing + \frac{2}{3}\ominus.
\end{aligned}$$

At this level, the identity is quite trivial. Let us therefore also check the relation at the three-loop level:

$$\begin{aligned}
[s(\varnothing), s(\ominus)] \varnothing &= s(\varnothing)s(\ominus) \varnothing - s(\ominus)s(\varnothing) \varnothing \\
&= s(\varnothing)(2\varnothing) - s(\ominus)\left(\frac{2}{3}\varnothing + \frac{2}{3}\varnothing + \frac{2}{3}\varnothing\right) \\
&= 2\left(\frac{2}{3}\varnothing + \frac{1}{3}\varnothing + \frac{2}{3}\varnothing + \frac{2}{3}\varnothing + \frac{2}{3}\varnothing\right) \\
&\quad - \frac{2}{3}(4\varnothing + 2\varnothing + 2\varnothing + 2\varnothing + 2\varnothing) \\
&= \frac{4}{3}\varnothing + \frac{2}{3}\varnothing - \frac{4}{3}\varnothing - \frac{4}{3}\varnothing - \frac{4}{3}\varnothing
\end{aligned}$$

but

$$\begin{aligned}
s([\varnothing, \ominus]) \varnothing &= s\left(\frac{1}{3}\varnothing + \frac{2}{3}\ominus - 2\varnothing\right) \varnothing \\
&= \frac{1}{3}(2\varnothing) + \frac{2}{3}(2\varnothing) - 2\left(\frac{2}{3}\varnothing + \frac{2}{3}\varnothing + \frac{2}{3}\varnothing\right) \\
&= \frac{4}{3}\varnothing + \frac{2}{3}\varnothing - \frac{4}{3}\varnothing - \frac{4}{3}\varnothing - \frac{4}{3}\varnothing.
\end{aligned}$$

Here we see that cancellation of graphs  and  was necessary in the first bracket, which is to be expected since these two graphs are generated by “mutually nonlocal” insertions, as defined above.

To summarize, if we know the commutator of two insertions, the identity (3) gives us the insertion of the commutator. A more concrete expression of this will be seen in section 5.2.

5.1 Connection with the Star Operation

The Ihara bracket identity can be compared to the star product discussed by Kreimer [30].

Here is the connection between our operator s_t and Kreimer’s star insertion \star :

$$t_1 \star t_2 \sim s(t_2) t_1$$

where the \sim alerts the reader that we use a different normalization, (1).

Furthermore,

$$(t_1 \star t_2) \star t_3 \sim s(t_3) s(t_2) t_1 \tag{5}$$

$$t_1 \star (t_2 \star t_3) \sim s(s(t_3) t_2) t_1 . \tag{6}$$

The coproduct Δ of the Connes-Kreimer Hopf algebra is coassociative, so the dual Hopf algebra should have an associative multiplication \odot . One would then naively expect the dual Lie algebra to have an associative multiplication as well. However, comparing (5) and (6), the star operation is not associative. This is because the original Hopf algebra contains disconnected graphs, but only connected graphs are generated by the star product (or equivalently, the grafting operator s_t). When the multiplication \odot is truncated to connected graphs, it is no longer associative.

The deviation from associativity can be measured by the *associativity defect*:

$$a(t_1 \mid t_2, t_3) \equiv t_1 \star (t_2 \star t_3) - (t_1 \star t_2) \star t_3 . \tag{7}$$

When this is nonzero, as in any nonassociative algebra, it is interesting to consider the “right-symmetric” algebra for which

$$a(t_1 \mid t_2, t_3) = a(t_1 \mid t_3, t_2) \tag{8}$$

(a “left-symmetric” algebra can equivalently be considered). This leads naturally to an algebra of the star product [30], which is also common usage in differential geometry. Writing the right-symmetric condition (8) explicitly in terms of the associativity defect (7), the algebra is specified by

$$t_1 \star (t_2 \star t_3) - (t_1 \star t_2) \star t_3 = t_1 \star (t_3 \star t_2) - (t_1 \star t_3) \star t_2 . \quad (9)$$

This is known as a *pre-Lie* (or *Vinberg*) algebra. A pre-Lie algebra yields a bracket $[t_1, t_2] = t_1 \star t_2 - t_2 \star t_1$ that automatically satisfies the Jacobi identity, hence “pre-Lie”. In our notation, using eqs. (5), (6), the pre-Lie algebra identity (9) can be rewritten as the operator identity (acting on arbitrary t_3):

$$[s(t_1), s(t_2)] = s([t_1, t_2]) , \quad (10)$$

that we have already shown directly for the grafting operator s_t . Thus the two descriptions are equivalent, as expected.

5.2 Matrix Representations

Graphs are graded by their number of loops, but there is no canonical ordering within each graded subspace. Given some ordering of graphs, the grafting operator s_t can be represented as a matrix. This matrix will be indexed by graphs. Now, graphs are inconvenient to use as subscripts, so we use a bra-ket notation instead: represent $s(t_1)t_2$ by

$$s(t_1)|t_2\rangle = \sum_{t_3} |t_3\rangle \langle t_3|s(t_1)|t_2\rangle$$

where all graphs are to be thought of as orthogonal: $\langle t_1|t_2\rangle = 0$ for $t_1 \neq t_2$.

An example: the insertion tables (consulting appendix A) gives

$$s(\mathfrak{X})\mathfrak{X} = \frac{2}{3}\mathfrak{X} + \frac{2}{3}\mathfrak{Y} + \frac{2}{3}\mathfrak{A} ,$$

which is to be compared to the expansion in a complete set

$$s(\mathfrak{X})|\mathfrak{X}\rangle = \dots + \langle \mathfrak{X}|s(\mathfrak{X})|\mathfrak{X}\rangle |\mathfrak{X}\rangle + \langle \mathfrak{Y}|s(\mathfrak{X})|\mathfrak{X}\rangle |\mathfrak{Y}\rangle + \langle \mathfrak{A}|s(\mathfrak{X})|\mathfrak{X}\rangle |\mathfrak{A}\rangle + \dots$$

so we read off

$$\langle \mathfrak{X}|s(\mathfrak{X})|\mathfrak{X}\rangle = 2/3 , \quad \langle \mathfrak{Y}|s(\mathfrak{X})|\mathfrak{X}\rangle = 2/3 , \quad \langle \mathfrak{A}|s(\mathfrak{X})|\mathfrak{X}\rangle = 2/3 .$$

giving the second column of the matrix:

$$s(\mathfrak{X})\mathfrak{X} \doteq \begin{pmatrix} 0 & 0 & 0 & 0 & 0 & 0 \\ 1/3 & 0 & 0 & 0 & 0 & 0 \\ 0 & 2/3 & 0 & 0 & 0 & 0 \\ 0 & 2/3 & 0 & 0 & 0 & 0 \\ 0 & 2/3 & 0 & 0 & 0 & 0 \\ 0 & 0 & 0 & 0 & 0 & 0 \end{pmatrix} \begin{pmatrix} 0 \\ 1 \\ 0 \\ 0 \\ 0 \\ 0 \end{pmatrix} = \begin{pmatrix} 0 \\ 0 \\ 2/3 \\ 2/3 \\ 2/3 \\ 0 \end{pmatrix} \doteq \frac{2}{3}\mathfrak{X} + \frac{2}{3}\mathfrak{X} + \frac{2}{3}\mathfrak{X} \quad (11)$$

where we have ordered the graphs as $\mathfrak{X}, \mathfrak{X}, \mathfrak{X}, \mathfrak{X}, \mathfrak{X}, \mathfrak{X}$, and \doteq denotes “represents”. In the appendix we give first insertion tables up to three-loop order (appendix A), then a few examples of matrices that represent the grafting operators (appendix B). These matrices are easily extracted from the insertion tables, and are indexed by graphs.

A word about practical implementation: because of our space-saving convention of suppressing graphs related by crossing symmetry, each number in the above 6×6 matrix is a 3×3 unit matrix, with the exception of the first row, which represents the tree-level diagram and so is a 3×1 matrix. Thus, in a completely explicit notation, the above matrix is 16×16 .

A few remarks are in order. It is immediately clear that the matrices s_t are all lower triangular, since insertion can never decrease loop number. (Recall that s_1 , which is represented by a diagonal matrix, is left out of the algebra). Triangularity makes these matrices easy to exponentiate, since the series will cut off at finite order. This property will be crucial in section 7. Triangular matrices are non-invertible, which makes sense—typically each application of s_t creates many different graphs. There is no unique inverse under s_t of a generic graph (but see section 6.1). Finally, by a quick glance in the appendix we see that the matrices are very sparse, which is useful to know for computer storage; the size of the matrix is the number of relevant diagrams squared, which quickly becomes prohibitive if sparsity is not exploited.

It will be useful in the following to consider exponentiating matrices, for example the matrix representing $s(\mathfrak{X})$ in (11):

$$\begin{aligned} \exp(s(\mathfrak{X}))\mathfrak{X} &= (1 + s(\mathfrak{X}) + \frac{1}{2}s(\mathfrak{X})s(\mathfrak{X}))\mathfrak{X} \\ &= \mathfrak{X} + \frac{1}{3}\mathfrak{X} + \frac{2}{3}\mathfrak{X} + \frac{2}{3}\mathfrak{X} + \frac{2}{3}\mathfrak{X} \end{aligned}$$

since the matrix (11) vanishes when cubed. On the other hand,

$$\exp(s(\mathfrak{X}))\mathfrak{X} = 0.$$

Thus, the exponential of the sum of all grafting operators acts as

$$e^{\sum_t s_t} \times = \times + \frac{1}{3} \text{\texttt{X}} + \frac{2}{3} \text{\texttt{X}} + \frac{2}{3} \text{\texttt{X}} + \frac{2}{3} \text{\texttt{X}} + \dots$$

where the dots denote higher-order terms. Acting with the inverse is now a simple matter:

$$e^{-\sum_t s_t} \times = \times - \frac{1}{3} \text{\texttt{X}} + \frac{2}{3} \text{\texttt{X}} + \frac{2}{3} \text{\texttt{X}} + \frac{2}{3} \text{\texttt{X}} + \dots \quad (12)$$

With the three-loop matrices given in the appendix, one easily performs exponentiation to three-loop level as well (see section 8). The alternating signs in equation (12) is already now suggestive for the reader who is familiar with Hopf algebra. The antipode of the Hopf algebra has a similar alternating sign—each shrinking of a subgraph comes with a sign change. In section 7 we display the relation to the antipode, and thus the counterterms of the theory.

6 Other Operations

6.1 Shrinking

When acting with the transpose of the matrix representation of a grafting operator, we shrink graphs. Here is an example:

$$s^T(\text{\texttt{X}})\text{\texttt{X}} \doteq \begin{pmatrix} 0 & 1/3 & 0 & 0 & 0 & 0 \\ 0 & 0 & 2/3 & 2/3 & 2/3 & 0 \\ 0 & 0 & 0 & 0 & 0 & 0 \\ 0 & 0 & 0 & 0 & 0 & 0 \\ 0 & 0 & 0 & 0 & 0 & 0 \\ 0 & 0 & 0 & 0 & 0 & 0 \end{pmatrix} \begin{pmatrix} 0 \\ 0 \\ 1 \\ 0 \\ 0 \\ 0 \end{pmatrix} = \begin{pmatrix} 0 \\ 2/3 \\ 0 \\ 0 \\ 0 \\ 0 \end{pmatrix} \doteq 2/3 \text{\texttt{X}}$$

This operation does not have a counterpart in the star notation; we will not explore it further here.

6.2 Gluing and External Leg Corrections

By insertion we only create 1-particle-irreducible (1PI) diagrams. We can also define the operation of *gluing*, that is, joining any two external legs of two graphs with a new propagator. Under this operation, either the insertion graph becomes an external leg correction to the object graph (if the insertion is has 2 external legs) or we add more external legs (if the insertion has n external legs with $n > 2$). In the latter case, we obtain n -point functions with $n > 4$, which are not superficially divergent in ϕ^4 theory, so we do not consider them.

As for the external leg correction, it does not have to be considered here either, since we only need amputated graphs for the S -matrix.

Thus, the gluing operation will not be of much direct interest to us, but it does have one property we wish to emphasize. Define $t_1 \circ t_2$ to be gluing of t_1 onto t_2 , e.g. $\mathfrak{X} \circ \underline{\mathfrak{O}}$ is an external leg correction to \mathfrak{X} . The operator s satisfies the Leibniz rule on these diagrams:

$$s(t_1)(t_2 \circ t_3) = (s(t_1)t_2) \circ t_3 + t_2 \circ (s(t_1)t_3) . \quad (13)$$

It is easy to check that this relation holds in examples in ϕ^4 theory.

The structure of (13) also seems to indicate a possible interpretation as a coderivation. We will not explore this direction in this work, since as we have seen, the gluing operation is not needed for computing S -matrix elements in our model field theory.

7 Renormalization

Consider a matrix M_1 depending on a parameter ϵ , with elements that diverge when $\epsilon \rightarrow 0$. Writing $M_1(1/\epsilon, \epsilon)$, we mean that both positive and negative powers of ϵ occur in the matrix elements. If only ϵ occurs in the argument and not $1/\epsilon$, there are no negative powers. We can decompose the divergent matrix M_1 into a finite part M_2 and a divergent part M_3 by the general procedure known as Birkhoff decomposition:

$$M_1(1/\epsilon, \epsilon) = M_2(1/\epsilon)M_3(\epsilon) , \quad (14)$$

which is uniquely fixed by a boundary condition $M_2(0) = 0$. The matrix M_3 has a limit as $\epsilon \rightarrow 0$. Birkhoff decomposition was applied to renormalization by Connes and Kreimer [20]. We take a somewhat different approach; those authors treat the three matrices in the decomposition (14) as the same type of objects, whereas we will use the Lie algebra to reduce M_1 and M_3 to vectors, but keep M_2 as a matrix. The main point is that we choose M_2 in the group corresponding to the Lie algebra of matrices defined in section 5.2. That is, the divergent matrix M_2 is a matrix C of the form

$$C = \exp \left(\sum_t C(t)s(t) \right)$$

with numerical coefficients $C(t)$ representing the overall divergence of the graphs t . In dimensional regularization, ϵ represents $\epsilon = 4 - D$ where D is the (complex) spacetime dimension. The boundary condition $M_2(0) = 0$ is realized in the MS scheme, but other

schemes can be accommodated by adapting other boundary conditions. The coefficient $C(t)$ will depend on ϵ so it should properly be denoted $C_\epsilon(t)$, however, we will suppress this dependence. The coefficient $C(t)$ is a polynomial in $1/\epsilon$ with no constant term (again, this is the boundary condition for (14)), but can depend on external momenta. To calculate the complete set of counterterms, it suffices to know these overall-divergence coefficients.

Let us describe the renormalization procedure in this framework, assuming we know the matrix C , i.e. both the overall-divergence values $C(t)$ and the combinatorial matrices s_t . Denote the bare value of a graph t by $B(t)$ and the renormalized graph by $A(t)$ (in the graph-by-graph method [16]). Vectors containing these values, indexed by graphs, are denoted A and B , respectively. We Birkhoff-decompose the vector of bare values as in equation (14):

$$B_{1/\epsilon, \epsilon} = C_{1/\epsilon} A_\epsilon .$$

To find renormalized values from bare values, we have to invert the matrix C , which is a trivial matter when it is expressed as an exponential:

$$\begin{aligned} A_\epsilon &= (C_{1/\epsilon})^{-1} B_{1/\epsilon, \epsilon} \\ &= \exp \left(- \sum_t C(t) s(t) \right) B_{1/\epsilon, \epsilon} . \end{aligned} \tag{15}$$

This is our main result. As we already pointed out, the sign in the exponential reproduces the sign of Zimmermann's forest formula [2], since every $s(t)$ factor in the expansion of the exponential corresponds to an insertion, and a sign.

This is most easily understood in an example. Let us calculate the renormalized 4-point function up to two loops:

$$\exp \left(- \sum_t C(t) s(t) \right) B = \begin{pmatrix} 1 & 0 & 0 & 0 & 0 & 0 \\ -C(\text{X}) & 1 & 0 & 0 & 0 & 0 \\ -C(\text{Y}) & -2C(\text{X}) & 1 & 0 & 0 & 0 \\ -C(\text{Z}) & -2C(\text{X}) & 0 & 1 & 0 & 0 \\ -C(\text{W}) & -2C(\text{X}) & 0 & 0 & 1 & 0 \\ -C(\text{V}) & -2C(\text{X}) & 0 & 0 & 0 & 1 \end{pmatrix} \begin{pmatrix} B(\text{X}) \\ B(\text{Y}) \\ B(\text{Z}) \\ B(\text{W}) \\ B(\text{W}) \\ B(\text{V}) \end{pmatrix}$$

where we, as mentioned earlier, use a symmetric renormalization point so that $C(\text{X}) = C(\text{Y}) = C(\text{Z})$. In fact, these three graphs always appear in the same place in the expansion,

since $s(\text{X}) = s(\text{Y}) = s(\text{Z})$. We have, for the nontrivial elements,

$$\begin{pmatrix} A(\text{X}) \\ A(\text{Y}) \\ A(\text{Z}) \\ A(\text{A}) \\ A(\text{B}) \end{pmatrix} = \begin{pmatrix} -C(\text{X})B(\text{X}) + B(\text{X}) \\ -C(\text{Y})B(\text{X}) - 2C(\text{X})B(\text{Y}) + B(\text{Y}) \\ -C(\text{Z})B(\text{X}) - 2C(\text{X})B(\text{Z}) + B(\text{Z}) \\ -C(\text{A})B(\text{X}) - 2C(\text{X})B(\text{A}) + B(\text{A}) \\ -C(\text{B})B(\text{X}) - 2C(\text{B})B(\text{Z}) + B(\text{Z}) \end{pmatrix}$$

To be specific, consider the third row:

$$A(\text{Z}) = -C(\text{Z})B(\text{X}) - 2C(\text{X})B(\text{Z}) + B(\text{Z}) , \quad (16)$$

where we, as mentioned earlier, use a symmetric renormalization point so that $C(\text{X}) = C(\text{Y}) = C(\text{Z})$. The combination of graphs is clearly correct; the second counterterm cancels the potentially nonlocal divergence in Z , and the first counterterm takes care of the overall divergence after the nonlocal one is canceled. The matrix C “knew” the connection between a graph and its divergent subgraphs, since C was constructed from the grafting operators s_t . We need to check the combinatorial factor of 2 in (16). Evaluating now in ϕ^4 theory (putting the overall counterterm $C(\text{X})$ aside for the moment):

$$\begin{aligned} A(\text{Z}) &= -2 \cdot \frac{\lambda^2}{2(4\pi)^2} \left(\frac{2}{\epsilon} - \ln M^2 + \text{finite} \right) \times \frac{1}{2} \left(\frac{2}{\epsilon} - \ln(-p^2) + \text{finite} \right) \\ &\quad + \frac{\lambda^2}{2(4\pi)^2} \cdot \frac{2}{\epsilon} \left(\frac{1}{\epsilon} - \ln(-p^2) + \text{finite} \right) . \end{aligned}$$

Again, we use a symmetric renormalization point $s = t = u = -M^2$, and included the symmetry factors of 1/2. We see that the combinatorial 2 assures cancellation of $(1/\epsilon) \ln(-p)^2$. The second order vertex counterterm $C(\text{Z})B(\text{X})$ takes care of the momentum-independent poles in ϵ . The total contribution to the 4-point function up to two-loop order is just the sum of all compatible (4-external-leg) elements of A , as in

$$\begin{aligned} \mathcal{A} &= A(\text{X}) + A(\text{Y}) + A(\text{Z}) + A(\text{A}) + A(\text{B}) \quad (+\text{crossing}) \\ &= B(\text{X}) - C(\text{X})B(\text{X}) + B(\text{Y}) \\ &\quad - C(\text{Y})B(\text{X}) - 2C(\text{X})B(\text{Y}) + B(\text{Z}) - C(\text{Z})B(\text{X}) - 2C(\text{X})B(\text{Z}) + \\ &\quad B(\text{A}) - C(\text{A})B(\text{X}) - 2C(\text{X})B(\text{A}) + B(\text{B}) \\ &= B(\text{X}) + B(\text{Y}) + B(\text{Z}) + B(\text{A}) + B(\text{B}) \\ &\quad - (C(\text{X}) + C(\text{Y}) + C(\text{Z}) + C(\text{A}))B(\text{X}) - 6C(\text{X})B(\text{Y}) . \end{aligned}$$

In some applications, we may consider absorbing the combinatorial factors into the graphs, since the Lie algebra is still satisfied if we simultaneously drop the overall normalization and multiplicities (cf. [30]).

8 Three-loop Example

All the diagrams at 3-loop order in ϕ^4 theory have been computed, and clever techniques have been invented to perform the computations. Some techniques are reviewed in [13]. A useful reference for tables of divergent parts up to three loops is [15]. Therefore, we need only worry about the combinatorics, but we still find it useful to indicate which integral computation techniques can be used to compute the relevant diagrams.

In one-loop computations, one usually employs the method of Feynman parameters. In fact, using Feynman parameters without additional techniques is, by some estimates, only economical for graphs with two lines. “Additional techniques” can include performing some series expansions before computing the integral (the Gegenbauer polynomials have been shown to be well suited for this), and imaginative use of integration by parts. In this context, integration by parts is applied to simplify integrals using the vanishing of integrals over total derivatives:

$$\int d^4p \frac{\partial}{\partial p} I(p) = 0$$

for any integrand $I(p)$ depending on the loop momentum p and any other loop or external momenta. Applying integration by parts, the massive ladder diagram \boxtimes at zero momentum transfer can be decomposed as [11]

$$\begin{aligned} \boxtimes \xrightarrow{I} & \frac{1}{(4\pi)^4} \left(\frac{m^2}{4\pi M^2} \right)^{-\epsilon} \int \frac{d^D k}{(2\pi)^D} \frac{[F(k^2)]^2}{(k^2 + m^2)} \\ & + \frac{1}{\epsilon} \frac{4}{(4\pi)^2} \left(\frac{m^2}{4\pi M^2} \right)^{-\epsilon/2} W_6 - \frac{1}{\epsilon^2} \frac{4}{(4\pi)^2} \left(\frac{m^2}{4\pi M^2} \right)^{-\epsilon} S_3, \end{aligned}$$

where F is a simpler genuine three-loop integral, i.e. it cannot be expressed in terms of integrals of lower loop order, W_6 is a two-loop integral (\boxtimes at zero momentum transfer) and S_3 is a one-loop integral (\boxtimes at zero momentum transfer). The result (given in [15]) is

$$\begin{aligned} \boxtimes \xrightarrow{I} & \frac{m^4}{(4\pi)^6} \left(\frac{m^2}{4\pi M^2} \right)^{-3\epsilon/2} \left(\frac{8}{3\epsilon^3} + \frac{1}{\epsilon^2} \left[\frac{8}{3} - 4\gamma \right] \right. \\ & \left. + \frac{1}{\epsilon} \left[\frac{4}{3} - 4a - 4\gamma + 3\gamma^2 + \frac{\pi^2}{6} \right] \right) + (\text{finite}) \end{aligned}$$

where γ is Euler’s constant, a is a numerical constant ($a = 1.17\dots$) coming from integration over Feynman parameters, and M is the renormalization scale.

Now let us use the matrix Lie algebra to compute the renormalized graph (again working in the graph-by-graph context). From the previous section, we know that counterterms are generated by the exponential of a sum over grafting operators.

Using

$$A = \exp \left[- (C(\varnothing)s(\varnothing) + C(\mathfrak{X})s(\mathfrak{X}) + C(\mathfrak{Y})s(\mathfrak{Y}) + \dots) \right] B ,$$

we find the renormalized graphs. In particular, the relevant row of the vector A is

$$\begin{aligned} A(\varnothing) &= \left(-\frac{2}{3} C(\varnothing)^3 + \frac{1}{2} C(\varnothing)C(\mathfrak{X}) - C(\varnothing\mathfrak{X}) \right) B(\mathfrak{X}) + \\ &\quad 2 C(\varnothing)^2 B(\mathfrak{X}) - C(\varnothing)B(\mathfrak{Y}) - C(\varnothing)B(\mathfrak{Z}) + B(\varnothing\mathfrak{X}) . \end{aligned} \quad (17)$$

This is to be compared to the known result for the renormalized graph:

$$\begin{aligned} \varnothing \Big|_{\text{ren}} &= \varnothing + (-\langle \varnothing \rangle + \langle \langle \varnothing \rangle \mathfrak{X} \rangle + \langle \langle \varnothing \rangle \mathfrak{Z} \rangle - \langle \langle \varnothing \rangle \langle \varnothing \rangle \mathfrak{X} \rangle) \\ &\quad - \langle \mathfrak{X} \rangle \mathfrak{X} - \langle \mathfrak{X} \rangle \mathfrak{Z} + \langle \mathfrak{X} \rangle^2 \langle \mathfrak{X} \rangle \end{aligned} \quad (18)$$

where $\langle \rangle$ denotes the renormalization map (for example, in minimal subtraction we simply drop the finite part). Rewriting the known expression (18) in language more similar to the above, we have

$$\begin{aligned} A(\varnothing) &= B(\varnothing) + (-C(\varnothing) + C(\varnothing)C(\mathfrak{X}) + C(\varnothing)C(\mathfrak{Z}) - C(\varnothing)^2 C(\mathfrak{X})) B(\mathfrak{X}) \\ &\quad - C(\mathfrak{X})B(\mathfrak{X}) - C(\mathfrak{X})B(\mathfrak{Z}) + C(\mathfrak{X})^2 B(\mathfrak{X}) . \end{aligned}$$

Upon dropping the combinatorial factors in (17), expression (18) is reproduced by that derived by the Lie algebra. We would like to understand better why the combinatorial factors do not match up in this example; perhaps our space-saving convention (section 7) causes some discrepancy. To summarize, we have used the inverse exponential of Lie algebra elements to generate counterterms, just as the antipode would have been used in a Hopf algebra.

The Ihara bracket relation $s_{[t_1, t_2]} = [s_{t_1}, s_{t_2}]$ is still rather trivial in this example, as it turns out, because only $s(\varnothing)$ appears more than once. In the example of \mathfrak{X} , we have $s(\varnothing)$, $s(\mathfrak{X})$ and $s(\mathfrak{Y})$ appearing, so there is potential for use of the relation here. However, the only nontrivial commutator, equation (4), yields graphs that do not appear as subgraphs of \mathfrak{X} :

$$\frac{1}{3} s(\underline{\mathfrak{X}}) + \frac{2}{3} s(\ominus) - 2 s(\mathfrak{X}) = [s(\varnothing), s(\underline{\mathfrak{X}})] .$$

We have thus seen that it is not until the four-loop level that nontrivial application of the Lie algebra relation $s_{[t_1, t_2]} = [s_{t_1}, s_{t_2}]$ appear. This will be pursued in future work. As mentioned in the introduction, new results are needed at five loops and higher.

9 Renormalization Group Flows and Nonrenormalizable Theories

In Wilson’s approach to renormalization, short-distance (ultraviolet) fluctuations are integrated out of the functional integral to appear only as modifications of parameters of the Lagrangian for the remaining long-distance (infrared) degrees of freedom [38]. The introduction of a mass scale M by renormalization parameterizes different renormalization schemes, and the change of M induces a flow of parameters in the Lagrangian, such that certain so-called irrelevant operators die away. In ϕ^4 theory in four dimensions, ϕ^6 is an example of one such operator; the relative size of this operator to other terms in the Lagrangian at a momentum scale p would be $(p/\Lambda)^{6-D} = (p/\Lambda)^2$ as $p \rightarrow 0$, where Λ is a cutoff.

Now, the grafting operator s_t may be thought of as a “magnifying glass”; by inserting graphs, we resolve details of graphs that were not visible at larger scales. In this specific sense, s_t induces scale change. (For a more speculative geometrical point of view, see the next section). In particular, in this paper, we only considered s_t for graphs t with 2 or 4 external legs. We do not have to consider s_t for graphs with 6 or more external legs in ϕ^4 theory in four dimensions, exactly because ϕ^6 is an irrelevant operator. This shows how the matrix Lie algebra would appear in a nonrenormalizable theory; everything is the same as in the ϕ^4 example, except there is an infinite number of insertion matrices. While this situation is certainly more cumbersome, it is not necessarily fatal.

According to Connes and Kreimer [20], renormalization group flow boils down to the calculation of a matrix β which in our notation becomes

$$\beta = \sum_t \beta(t) s_t ,$$

and is independent of ϵ . Here $\beta(t)$ is the numerical contribution to the beta function due to a certain diagram t (again, in the graph-by-graph method). This matrix β generalizes the standard beta function of the renormalization group; there is now combinatorial information attached to each of the contributions $\beta(t)$ to the beta function.

See also the next section for some comments on the validity of Wilson’s point of view.

10 Conclusion and Outlook

In this work, we displayed a matrix Lie algebra of operators acting on Feynman graphs, that by exponentiation yields group elements generating counterterms for diagrams with subdivergences. We defined a grafting operator s_t that inserts one Feynman graph t into another. The matrix representations of these operators satisfy a certain rule, similar to an Ihara bracket, that gives relations between them: $s_{[t_1, t_2]} = [s_{t_1}, s_{t_2}]$. In this way, not all matrices have to be separately computed, with potentially substantial savings in computation time. We displayed the relation to the star product of Kreimer, which is defined similarly to (but not exactly the same way as) the grafting operator. A simple computation verifies that the right-symmetric (pre-Lie) nonassociative algebra of the star product is equivalent to the previously mentioned Ihara-bracket rule for our matrix representations.

We also gave a number of examples, mostly rather simple ones, and checked in a three-loop example that the correct sequence of counterterms is provided by the exponential of Lie algebra elements. (The general proof that this is always the case will be given elsewhere [6]). Just as with Hopf algebra, the Lie algebra rules are trivial at one-loop, almost trivial at two-loop, and just beginning to become interesting at three-loop order. At four loops, there is plenty of interesting structure to check, but it will require a large-scale computation effort; this is an obvious direction in which future work should go.

An equally obvious, but less direct, application is to noncommutative geometry. Using the Connes-Kreimer homomorphism between the Hopf algebra of renormalization and the Hopf algebra of coordinates on the group of formal diffeomorphisms [20, 22], and the Milnor-Moore theorem, the Lie algebra in this paper has a corresponding Lie algebra in the context of noncommutative geometry. We hope that the matrix Lie algebra may eventually shed some light on certain aspects of noncommutative geometry, in this rather indirect but novel way.

In a less obvious direction, it is suggestive to note that the grafting operator s_t is an element of a Lie algebra, it satisfies a Leibniz rule (the gluing operator, section 6.2), and its bracket (3) looks like that of a vector field X on a manifold. Loosely, the grafting operator is a “scale vector”, that takes us into ever increasing magnification of graphs by including more and more subgraphs. If a Lie derivative \mathcal{L}_{s_t} along this “vector field” could meaningfully be defined, that would open the following interesting speculative possibility.

It was proposed in [8], based on earlier work [7] that volume forms for functional integration be characterized the following way: find a vector field X on the space, define

its divergence (this may be a nontrivial task in an infinite-dimensional space) and let the volume form ω be defined by

$$\mathcal{L}_X \omega = (\operatorname{div} X) \omega .$$

This definition reproduces familiar volume forms in some simple finite-dimensional examples (Riemannian manifolds, symplectic manifolds), and gives some hope for generalization to infinite-dimensional spaces. Perhaps if s_t is a vector field, it could be used in the role of X , in some extended sense, to characterize ω . In effect, this would be a perturbative definition, since including s_t up to a certain loop order will define different ω at different orders in the loop expansion.

An obvious problem with this idea is that s_t acts on the space of *graphs*, not the space of fields. This means that even if a volume form ω could be defined, it would be a function on the space of graphs. In principle, it may be possible to exploit some analogy to the space of paths in quantum-mechanical functional integrals. This direction would be interesting to pursue in future work.

As a final note, there has been some dispute to what extent Wilson's picture is generally valid; there are some (as yet speculative) examples where infrared and ultraviolet divergences are connected [34]. Some of these examples are in connection with noncommutative geometry. In view of the relation between the algebraic approach to renormalization and noncommutative geometry mentioned above, one could hope that these algebraic developments may eventually shed some light on the ultraviolet-infrared connection.

11 Acknowledgments

We wish to thank C. DeWitt-Morette, D. Kreimer and A. Wurm for useful and pleasant discussions. MB wishes to thank the Swedish Foundation for International Cooperation in Research and Higher Education for financial support, and the Departement de Mathématiques et Applications, Ecole Normale Supérieure, Paris, for hospitality.

A Insertion Tables

In this appendix, we provide tables of the action of the grafting operator s_t . We have defined s_t such that on a bare diagram denoted by 1, we have $s_t 1 = t$. The matrix s_1 acts as $s_1 t = N(t)t$ where $N(t)$ is the number of insertion points of t . It is also true that the coefficients of each resulting graph in an insertion into a graph t should add up to the number of compatible insertion points of the graph t .

One-loop:

$$1 + 0 = 1$$

$$s(\underline{\circ}) - = \underline{\circ}$$

$$s(\underline{\circ}) \times = 0$$

$$s(\overline{\circ}) - = 0$$

$$s(\overline{\circ}) \times = \frac{1}{3} \overline{\circ} + \text{crossing}$$

Two-loop:

$$1 + 1 = 2$$

$$s(\underline{\circ}) \underline{\circ} = \underline{\circ}$$

$$s(\underline{\circ}) \overline{\circ} = 2 \overline{\circ}$$

$$s(\overline{\circ}) \underline{\circ} = \frac{1}{3} \underline{\circ} + \frac{2}{3} \ominus$$

$$s(\overline{\circ}) \overline{\circ} = \frac{2}{3} \overline{\circ} + \frac{2}{3} \overline{\circ} + \frac{2}{3} \overline{\circ}$$

Three-loop:

$$1 + 2 = 3$$

$$s(\underline{\circ}) \underline{\circ} = 2 \overline{\circ} + \underline{\circ}$$

$$s(\underline{\circ}) \overline{\circ} = 4 \overline{\circ}$$

$$s(\underline{\circ}) \overline{\circ} = 2 \overline{\circ} + 2 \overline{\circ}$$

$$s(\underline{\circ}) \overline{\circ} = 2 \overline{\circ} + 2 \overline{\circ}$$

$$s(\underline{\circ}) \overline{\circ} = \frac{4}{3} \overline{\circ} + \frac{4}{3} \overline{\circ} + \frac{4}{3} \overline{\circ}$$

$$s(\overline{\circ}) \underline{\circ} = \frac{2}{3} \underline{\circ} + \frac{2}{3} \underline{\circ} + \frac{2}{3} \ominus$$

$$s(\text{X}) \ominus = 2 \text{X}$$

$$s(\text{X}) \text{X} = \frac{2}{3} \text{X} + \text{X} + \frac{2}{3} \text{X} + \frac{2}{3} \text{X}$$

$$s(\text{X}) \text{X} = \frac{1}{3} \text{X} + \frac{1}{3} \text{X} + \frac{2}{3} \text{X} + \frac{1}{3} \text{X} + \frac{2}{3} \text{X} + \frac{2}{3} \text{X}$$

$$s(\text{X}) \text{X} = \frac{1}{3} \text{X} + \frac{1}{3} \text{X} + \frac{2}{3} \text{X} + \frac{1}{3} \text{X} + \frac{2}{3} \text{X} + \frac{2}{3} \text{X}$$

$$s(\text{X}) \text{X} = \frac{2}{3} \text{X} + \frac{1}{3} \text{X} + \frac{2}{3} \text{X} + \frac{2}{3} \text{X} + \frac{2}{3} \text{X}$$

$$2 + 1 = 3$$

$$s(\text{X}) \text{X} = \text{X}$$

$$s(\text{X}) \text{X} = \text{X}$$

$$s(\text{X}) \text{X} = 2 \text{X}$$

$$s(\text{X}) \text{X} = 2 \text{X}$$

$$s(\text{X}) \text{X} = \frac{1}{3} \text{X} + \frac{2}{3} \text{X}$$

$$s(\text{X}) \text{X} = \frac{2}{3} \text{X} + \frac{1}{6} \text{X} + \frac{1}{6} \text{X}$$

$$s(\text{X}) \text{X} = \frac{2}{3} \text{X} + \frac{1}{6} \text{X} + \frac{1}{6} \text{X}$$

$$s(\text{X}) \text{X} = \frac{1}{3} \text{X} + \frac{2}{3} \text{X}$$

$$s(\text{X}) \text{X} = \frac{2}{3} \text{X} + \frac{2}{3} \text{X} + \frac{2}{3} \text{X}$$

$$s(\text{X}) \text{X} = \frac{1}{3} \text{X} + \frac{1}{6} \text{X} + \frac{1}{6} \text{X} + \frac{1}{3} \text{X} + \frac{1}{3} \text{X} + \frac{1}{3} \text{X} + \frac{1}{3} \text{X}$$

$$s(\text{X}) \text{X} = \frac{1}{3} \text{X} + \frac{1}{6} \text{X} + \frac{1}{6} \text{X} + \frac{1}{3} \text{X} + \frac{1}{3} \text{X} + \frac{1}{3} \text{X} + \frac{1}{3} \text{X}$$

B Grafting Matrices

In this appendix, we list matrix representations of the grafting operators $s(t)$. Since insertion into an n -point function can only create an n -point function, we consider submatrices of

each separately, and denote them by subscripts. For example, if we call $s(\mathfrak{X})_- = A$ and $s(\mathfrak{X})_{\times} = B$, then the complete matrix representing $s(\mathfrak{X})$ is the direct sum of A and B :

$$s(\mathfrak{X}) \doteq \left(\begin{array}{c|c} A & 0 \\ \hline 0 & B \end{array} \right).$$

Lines are drawn through the matrices to delineate loop order L .

One-loop insertions:

$$\begin{aligned} s(\mathfrak{Q})_- &= \left(\begin{array}{c|c|c|c} 0 & 0 & 0 & 0 \\ \hline 1 & 0 & 0 & 0 \\ \hline 0 & 1 & 0 & 0 \\ \hline 0 & 0 & 0 & 0 \end{array} \right) \begin{array}{l} - \\ \mathfrak{Q} \\ \mathfrak{R} \\ \ominus \end{array} & s(\mathfrak{X})_- &= \left(\begin{array}{c|c|c|c} 0 & 0 & 0 & 0 \\ \hline 0 & 0 & 0 & 0 \\ \hline 0 & \frac{1}{3} & 0 & 0 \\ \hline 0 & \frac{2}{3} & 0 & 0 \end{array} \right) \begin{array}{l} - \\ \mathfrak{Q} \\ \mathfrak{R} \\ \ominus \end{array} \\ \\ s(\mathfrak{Q})_{\times} &= \left(\begin{array}{c|c|c|c|c|c} 0 & 0 & 0 & 0 & 0 & 0 \\ \hline 0 & 0 & 0 & 0 & 0 & 0 \\ \hline 0 & 0 & 0 & 0 & 0 & 0 \\ \hline 0 & 0 & 0 & 0 & 0 & 0 \\ \hline 0 & 0 & 0 & 0 & 0 & 0 \\ \hline 0 & 2 & 0 & 0 & 0 & 0 \end{array} \right) \begin{array}{l} \times \\ \mathfrak{X} \\ \mathfrak{X} \\ \mathfrak{X} \\ \mathfrak{X} \\ \mathfrak{X} \end{array} & s(\mathfrak{X})_{\times} &= \left(\begin{array}{c|c|c|c|c|c} 0 & 0 & 0 & 0 & 0 & 0 \\ \hline \frac{1}{3} & 0 & 0 & 0 & 0 & 0 \\ \hline 0 & \frac{2}{3} & 0 & 0 & 0 & 0 \\ \hline 0 & \frac{1}{3} & 0 & 0 & 0 & 0 \\ \hline 0 & \frac{2}{3} & 0 & 0 & 0 & 0 \\ \hline 0 & 0 & 0 & 0 & 0 & 0 \end{array} \right) \begin{array}{l} \times \\ \mathfrak{X} \\ \mathfrak{X} \\ \mathfrak{X} \\ \mathfrak{X} \\ \mathfrak{X} \end{array} \end{aligned}$$

When it comes to three-loop matrices, it is typographically easier to give the transpose:

$$s^T(\mathfrak{X})_{\times} = \left(\begin{array}{cccccccccccccccccccccccccccccccc} 0 & 0 \\ \hline 0 & 0 \\ \hline 0 & 0 & 0 & \frac{2}{3} & 1 & 0 & 0 & \frac{2}{3} & \frac{2}{3} & 0 & 0 & 0 & 0 & 0 & 0 & 0 & 0 & 0 & 0 & 0 & 0 & 0 \\ \hline 0 & 0 & \frac{1}{3} & \frac{1}{3} & 0 & \frac{2}{3} & 0 & \frac{1}{3} & 0 & \frac{2}{3} & 0 & \frac{2}{3} & 0 & 0 & 0 & 0 & 0 & 0 & 0 & 0 & 0 & 0 \\ \hline 0 & 0 & \frac{1}{3} & \frac{1}{3} & 0 & 0 & \frac{2}{3} & 0 & \frac{1}{3} & 0 & \frac{2}{3} & 0 & \frac{2}{3} & 0 & 0 & 0 & 0 & 0 & 0 & 0 & 0 & 0 \\ \hline 0 & 0 & 0 & 0 & 0 & 0 & 0 & 0 & 0 & 0 & 0 & 0 & 0 & \frac{2}{3} & \frac{1}{3} & 0 & 0 & \frac{2}{3} & \frac{2}{3} & \frac{2}{3} & 0 & 0 \end{array} \right) \begin{array}{l} \times \\ \mathfrak{X} \\ \mathfrak{X} \\ \mathfrak{X} \\ \mathfrak{X} \\ \mathfrak{X} \\ \mathfrak{X} \end{array}$$

where all elements below those displayed are zero (it is, of course, a square matrix), and we have not displayed the zero-one-two-loop submatrices already given. That is, the given matrix is the transpose of the 22×6 submatrix B in

$$\left(\begin{array}{c|c} A & 0 \\ \hline B & 0 \end{array} \right),$$

where A is the 6×6 matrix given for $s(\text{X})$ earlier. The order is as in table 1, summarized here:

1	2	3	4	5	6	7	8	9	10	11
12	13	14	15	16	17	18	19	20	21	22

We also give two two-loop insertions:

$$s^T(\text{X})_{\text{X}} = \begin{pmatrix} 0 & 0 \\ 0 & 0 & 0 & 0 & \frac{2}{3} & \frac{2}{3} & \frac{2}{3} & 0 & 0 & 0 & 0 & 0 & 0 & 0 & 0 & 0 & 0 & 0 & 0 & 0 & 0 & 0 \\ 0 & 0 \\ 0 & 0 \\ 0 & 0 \\ 0 & 0 \end{pmatrix} \begin{matrix} \text{X} \\ \text{X} \\ \text{X} \\ \text{X} \\ \text{X} \\ \text{X} \end{matrix}$$

$$s^T(\text{X})_{\text{X}} = \begin{pmatrix} 0 & 0 \\ 0 & 0 & 0 & \frac{1}{3} & 0 & 0 & 0 & \frac{1}{6} & \frac{1}{6} & \frac{1}{3} & \frac{1}{3} & \frac{1}{3} & \frac{1}{3} & 0 & 0 & 0 & 0 & 0 & 0 & 0 & 0 & 0 \\ 0 & 0 \\ 0 & 0 \\ 0 & 0 \\ 0 & 0 \end{pmatrix} \begin{matrix} \text{X} \\ \text{X} \\ \text{X} \\ \text{X} \\ \text{X} \\ \text{X} \end{matrix}$$

The rest of the matrices are now trivial to extract from the insertion tables, so we shall not repeat them here.

References

- [1] D. Becirevic, Ph. Boucaud, J.P. Leroy, J. Micheli, O. Pène, J. Rodríguez-Quintero, C. Roiesnel, *Asymptotic scaling of the gluon propagator on the lattice*, Phys.Rev. **D61** (2000) 114508; hep-ph/9910204.
- [2] N.N. Bogoliubov, O.S. Parasiuk, *Über die Multiplikation der Kausalfunktionen in der Quantentheorie der Felder*, Acta Math. **97** (1957) 227; K. Hepp, *Proof of the Bogoliubov-*

- Parasiuk Theorem of Renormalization*, Commun. Math. Phys. **2** (1966) 301; W. Zimmermann, in S. Deser et. al. eds, *Lectures on Elementary Particles and Quantum Field Theory, Vol I* (MIT Press, Cambridge, 1970).
- [3] D.J. Broadhurst, D. Kreimer, *Renormalization automated by Hopf algebra*, J. Symb. Comput. **27** (1999) 581; hep-th/9810087.
 - [4] D.J. Broadhurst, D. Kreimer, *Combinatoric explosion of renormalization tamed by Hopf algebra: 30-loop Padé-Borel resummation*, Phys. Lett. **B475** (2000) 63-70; hep-th/9912093.
 - [5] D.J. Broadhurst, D.Kreimer, *Exact solutions of Dyson-Schwinger equations for iterated one-loop integrals and propagator-coupling duality*, Nucl. Phys. **B600** (2001) 403-422.
 - [6] P. Cartier, to be published.
 - [7] P. Cartier, C. DeWitt-Morette, *A new perspective on functional integration*, J. Math. Phys **36** (1995) 2237-2312. P. Cartier, C. DeWitt-Morette, *Functional integration*, J. Math. Phys **41** (2000) 4154-4187.
 - [8] P. Cartier, M. Berg, C. DeWitt-Morette, and A. Wurm, *Characterizing Volume Forms*, to appear in Hagen Kleinert's festschrift (World Scientific, 2001); math-ph/0012009.
 - [9] A.H. Chamseddine, A. Connes, *The Spectral Action Principle*, Commun. Math. Phys. **186** (1997) 731-750.
 - [10] F. Chapoton, *Un théorème de Cartier-Milnor-Moore-Quillen pour les bigèbres dendri-formes et les algèbres braces*; math.QA/0005253.
 - [11] K. Chetyrkin, M. Misiak and M. Münz, *Beta functions and anomalous dimensions up to three loops*, Nucl. Phys. **B518**, 473 (1998); hep-ph/9711266.
 - [12] K.G. Chetyrkin, T. Seidensticker, *Two Loop QCD Vertices and Three Loop MOM β functions*, Phys.Lett. **B495** (2000) 74-80; hep-ph/0008094.
 - [13] K.G. Chetyrkin, F.V. Tkachov, *Integration by parts: the algorithm to calculate beta functions in 4 loops*. Nucl. Phys. **B192** (1981) 159-204; K.G. Chetyrkin, A.H. Hoang, J.H. Kuhn, M. Steinhauser and T. Teubner, *QCD corrections to the e^+e^- cross section and the Z boson decay rate: concepts and results*, Phys. Rep. **277** (1996), 189-281.
 - [14] C. Chrysomalakos, H. Quevedo, M. Rosenbaum, J.D. Vergara, hep-th/0105259.

- [15] J.-M. Chung and B.K. Chung, *Calculation of a Class of Three-Loop Vacuum Diagrams with Two Different Mass Values*, Phys. Rev. **D59** (1999) 105014; hep-ph/9805432.
- [16] J. C. Collins, *Renormalization* (Cambridge, 1985).
- [17] A. Connes, *A Short Survey of Noncommutative Geometry*, J. Math. Phys. **41** (2000) 3832-3866; hep-th/0003006.
- [18] A. Connes, M.R. Douglas, A. Schwarz, *Noncommutative Geometry and Matrix Theory: Compactification on Tori*, J. High Energy Phys. **02** (1998) 003; hep-th/9711162.
- [19] A. Connes, D. Kreimer, *Renormalization in quantum field theory and the Riemann-Hilbert problem I: the Hopf algebra structure of graphs and the main theorem*, Commun. Math. Phys. **210** (2000) 249-273; hep-th/9912092.
- [20] A. Connes, D. Kreimer, *Renormalization in quantum field theory and the Riemann-Hilbert problem II: the β -function, diffeomorphisms and the renormalization group*, Commun. Math. Phys. **216** (2001) 215-241; hep-th/0003188.
- [21] A. Connes, D. Kreimer, *Lessons from Quantum Field Theory — Hopf Algebras and Spacetime Geometries*, Lett. Math. Phys. **48** (1999) 85-96; hep-th/9904044.
- [22] A. Connes, H. Moscovici, *Differentiable cyclic cohomology and Hopf algebraic structures in transverse geometry*; math.DG/0102167.
- [23] J.M. Gracia-Bondía, J.C. Várilly, H. Figueroa, *Elements of Noncommutative Geometry* (Birkhäuser, Boston, 2001).
- [24] T. Hahn, *Generating Feynman Diagrams and Amplitudes with FeynArts 3*, hep-ph/0012260. The FeynArts web site is www.feynarts.de.
- [25] S. Heinemeyer, *Two-loop Calculations in the MSSM with FeynArts*, hep-ph/0102318.
- [26] C. Kassel, *Quantum Groups* (Springer-Verlag, New York, 1995).
- [27] M. Kontsevich, *Operads and Motives in Deformation Quantization*, Lett.Math.Phys. **48** (1999) 35-72; math.QA/9904055.
- [28] D. Kreimer, *On the Hopf algebra structure of perturbative quantum field theories*, Adv. Theor. Math. Phys. **2** (1998) 303-334; q-alg/9707029.

- [29] D. Kreimer, *Shuffling Quantum Field Theory*, Lett. Math. Phys. **51** (2000) 179-191; hep-th/9912290.
- [30] D. Kreimer, *Combinatorics of (perturbative) quantum field theory*, to appear in Phys. Rep.; hep-th/0010059
- [31] D. Kreimer, *Knots and Feynman Diagrams*, (Cambridge, 2000).
- [32] D. Kreimer, to appear.
- [33] C.P. Martín, J.M. Gracia-Bondía and J.C. Várilly, *The Standard Model as a noncommutative geometry: the low energy regime*, Phys. Rep. **294** (1998) 363-406.
- [34] S. Minwalla, M. Van Raamsdonk, N. Seiberg, *Noncommutative Perturbative Dynamics*, J. High Energy Phys. **02** (2000) 020; hep-th/9912072; M. Van Raamsdonk, N. Seiberg, *Comments on Noncommutative Perturbative Dynamics*, J. High Energy Phys. **03** (2000) 035; hep-th/0002186; L. Griguolo, M. Pietroni, *Wilsonian Renormalization Group and the Non-Commutative IR/UV Connection*, hep-th/0104217.
- [35] T. Ohl, *Drawing Feynman Diagrams with LaTeX and Metafont*, Comput. Phys. Commun. **90** (1995) 340; hep-ph/9505351.
- [36] G. Racinet, *Séries génératrices non-commutatives de polyzêtas et associateurs de Drinfeld*, Ph.D thesis (Université de Amiens, 2000).
- [37] N. Seiberg, E. Witten, *String Theory and Noncommutative Geometry*, J. High Energy Phys. **9909** (1999) 032; hep-th/9908142.
- [38] K.G. Wilson, J. Kogut, *The Renormalization Group and the ϵ Expansion*, Phys. Rep **12** (1974) 75-200.